Polymer 49 (2008) 4406–4412

Contents lists available at ScienceDirect

Polymer

journal homepage: www.elsevier.com/locate/polymer

Chiral-nematic self-ordering of rodlike cellulose nanocrystals grafted with poly(styrene) in both thermotropic and lyotropic states

Jie Yi [a,b], Qunxing Xu [a], Xuefei Zhang [a,c], Hailiang Zhang [a,b,*]

[a] School of Chemistry, Xiangtan University, Xiangtan 411105, Hunan Province, PR China
[b] Key Laboratory of Low-Dimensional Materials and Application Technology of Ministry of Education, Xiangtan University, Xiangtan 411105, Hunan Province, PR China
[c] Key Laboratory of Environment-Friendly Chemistry and Applications of Ministry of Education, Xiangtan 411105, Hunan Province, PR China

ARTICLE INFO

Article history:
Received 5 March 2008
Received in revised form 3 July 2008
Accepted 5 August 2008
Available online 9 August 2008

Keywords:
Cellulose nanocrystals (CNC)
Poly(styrene)
Chiral nematic phase

ABSTRACT

Graft copolymers of rodlike cellulose nanocrystals (CNC) with poly(styrene) (PSt) were synthesized through atom transfer radical polymerization (ATRP). The hydroxyl groups on CNC were esterified with 2-bromoisobutyrylbromide to yield 2-bromoisobutyryloxy groups, which were used to initiate the polymerization of poly(styrene). The graft copolymers were characterized by thermogravimetric analysis (TGA), fourier transform infrared spectroscopy (FT-IR) and gel permeation chromatography (GPC). The size of the original CNC is 10–40 nm in width and 100–400 nm in length, which was characterized by atomic force microscopy (AFM). The thermal and liquid crystalline properties of the graft copolymers were investigated by differential scanning calorimeter (DSC) and polarizing optical microscope (POM). The graft copolymers exhibit fingerprint texture in both thermotropic and lyotropic states. In thermotropic state, the PSt-grafted CNC orient spontaneously in isotropic melt (PSt side chains acting as a solvent). The thermotropic liquid crystal phase behavior is similar to the lyotropic phase behavior.

1. Introduction

The rodlike cellulose nanocrystals (CNC) has attracted significant attention during the last decade [1]. The interest is due to their renewable nature, abundance, good mechanical properties and large specific surface area. More recently, there is an increased use of CNC as reinforcement in nanocomposites [2]. The reason why the cellulose whiskers can be used as a reinforcing phase in nanocomposite is that they have a high aspect ratio and high bending strength [3,4]. The size of CNC is mainly dependent on the source [5,6] and the acid hydrolysis conditions [7,8]. However, the formation of weak interfacial interactions between the natural fibers and the polymer matrix can lead to composite failure [9]. The most efficient way to improve their compatibility and adhesion to other composite material components is to modify the cellulose surface by controlled grafting with hydrophobic or hydrophilic monomers. Several researches have been made to modify the cellulose nanocrystals by grafting [10–12]. In addition, grafting of synthetic polymers on the filter paper [13–15] and other solid cellulose substrates [16,17] have been reported. To study the compatibility and adhesion between cellulose fibers and hydrophobic composite material components, poly(styrene) was grafted on Whatman filter paper by reversible addition-fragmentation chain transfer (RAFT) polymerization [18,19]. All the aforementioned PSt-grafted cellulose substrates are of micrometer-size scale rather than nanometer-size. In this paper, chemical modified rodlike cellulose nanocrystals with poly(styrene) by ATRP were investigated, which have a great potential application of nanocomposite materials [2].

The excellent reinforced nanocomposite materials are required to be highly ordered. The anisotropy is one of the most important factors to effect the performance of reinforced nanocomposite materials. The study of liquid crystalline phases behavior of CNC is helpful to design high performance inexpensive biodegradable nanocomposite materials. The cellulose whiskers are rigid rodlike particles, which have a strong tendency to align along a vector director. This rod alignment creates a macroscopic birefringence that can be directly observed through crossed polarizers. The phase separation phenomena and chiral-nematic texture of cellulose whisker suspensions were recently reviewed [1]. It was well known that chiral-nematic phase was formed above the critical concentration of the CNC suspension [10,20–27]. These investigations were confirmed by phase equilibrium theory for rodlike particles [28–31]. Theory predicted that rodlike objects could spontaneously form a stable ordered phase under appropriate circumstances. In general, the experimental observation of the lyotropic phase

* Corresponding author. Key Laboratory of Low-Dimensional Materials and Application Technology of Ministry of Education, Xiangtan University, Xiangtan 411105, Hunan Province, PR China. Tel.: +86 732 8293717; fax: +86 732 8293264.
E-mail address: hailiangzhang1965@yahoo.com.cn (H. Zhang).

0032-3861/$ – see front matter © 2008 Elsevier Ltd. All rights reserved.
doi:10.1016/j.polymer.2008.08.008

requires rodlike objects in the certain solution to orient spontaneously. However, lyotropic character was also observed in an isotropic melt. Lyotropic phases of rigid rod polymer above the T_m of the PCL (PCL acting as a solvent) have been reported [32]. Poly-(γ-*n*-alkyl D-g1utamate)s having long alkyl side chains form both lyotropic and thermotropic liquid crystal phases (alkyl side chains acting as a solvent) [33]. In this model, a stiff insoluble core was solubilized by long alkyl chains (the hairs) on its surface, and they were the so-called "hairy rod" polymers. Unfortunately none of these studies has been focused on CNC lyotropic phases in isotropic melt. The liquid crystal–polymer composites have potential application in displays, smart windows [34], optical films, security papers and the optical actuators or devices [35]. In this study, the liquid crystalline phases behaviors of PSt-grafted CNC were investigated in DMF and above melting temperatures of the side chains. This is the first instance that the grafting CNC spontaneously exhibits fingerprint texture in both lyotropic and thermotropic states.

2. Experimental section

2.1. Materials

1,1,4,7,10,10-Hexamethyltriethylenetetramine (HMTETA, Aldrich, 98%) was used as received. Styrene (Aldrich, 99%) was passed through a column of neutral aluminium oxide prior to use. 2-Bromoisobuturyl bromide (BIBB) (98%, Alfa) was freshly distilled at room temperature under vacuum. Triethylamine (TEA) was refluxed with tosyl chloride to remove the primary amines and secondary amines. Cu(I)Br was washed with acetic acid and ethanol and then dried under vacuum. 4-Dimethylaminopyridine (DMAP, Acros, 99%) and sulfuric acid (95–98%) were used as received. The filter papers were purchased from the Hangzhou Double Rings Filter Paper Co Ltd in China. All other solvents were purified prior to use.

2.2. Preparation of rodlike cellulose nanocrystals

The rodlike cellulose nanocrystals were prepared by acid catalyzed hydrolysis of natural cellulose fibers as described previously [24]. In this case, filter papers were ground to smaller than 20 mesh powder in a mill. The ground paper (20 g) was mixed with sulfuric acid (175 ml, 64%) and stirred at 45 °C for 1 h. The acid was removed by centrifugation, and then residual sulfuric acid was removed by dialysis with deionized water until neutrality was reached. The suspensions was freeze-dried and dried for 48 h in a vacuum at 50 °C to a constant weight.

2.3. Immobilization of ATRP initiator on rodlike cellulose nanocrystals

The dried rodlike cellulose nanocrystals (1.5 g) were added to a solution containing DMAP (3.6 g, 27.7 mmol), TEA (1.98 g, 25 mmol) and 3.0 ml of 2-bromoisobutyrylbromide (4 ml, 32 mmol) diluted in 100 ml of dry THF, and the reaction was allowed to proceed with stirring for 24 h at room temperature. Then the cellulose nanocrystals were firstly rinsed with ethanol (96%) and extracted with CH_2Cl_2 in a Soxhlet apparatus to remove any residual small molecules. The resulting product was oven-dried under vacuum at 50 °C to a constant weight.

2.4. The synthesis PSt-grafted CNC

The initiator-modified CNC (0.1 g), CuBr (28.3 mg, 0.1 mmol), HMTETA (20.9 μl, 0.1 mmol), and styrene (2.0 g, 19.2 mmol) were introduced into a dry glass tube. The glass tube was degassed with three freeze-pump-thaw cycles and then sealed under vacuum. The tube was then placed in a thermostated oil bath and left at 110 °C for 12 h. After the reaction was over, the final compound was diluted in methanol, strongly sonicated for 5 min, and then centrifuged. Such process would be proceeded for three times to remove unreacted monomer and ungrafted bulk poly(styrene). Finally the PSt-grafted CNC was further purified by Soxhlet extraction with CH_2Cl_2, and placed in a vacuum at 50 °C for 24 h.

2.5. Cleaving of PSt chain from cellulose backbone

Poly(styrene) chains were cleaved from the CNC surface under acidic conditions. In a typical acid hydrolysis experiment, 0.121 g of PSt-grafted CNC sample was immersed into a round-bottom flask containing 10 mL of 37% HCl and 25 mL of THF. The flask was stirred at 80 °C for 3 weeks until the CNC was completely dissolved. Following the completion of the reaction, the solvent mixture was evaporated using a rotary evaporator and dried at 50 °C in a vacuum oven. The resulting viscous liquid was dissolved in toluene and then extracted with a small amount of distilled water (10–15 mL). After separation of the water layer, the organic phase was dried under anhydrous sodium sulfate for 24 h. After filtration of the sodium salt, poly(styrene) chains were collected by complete evaporation of the solvent (toluene). The weight of dried poly-(styrene) product is 0.082 g. The weight percent of PSt in the PSt-grafted CNC is determined as 68 wt%. The poly(styrene) product was then dissolved in THF, and the molecular weight (M_n) and molecular weight distribution (M_w/M_n) were analyzed by GPC. The PSt grafting ratio was calculated using the following formula:

$$\text{The PSt grafting ratio}(\%) = \frac{\text{reacted Br}}{\text{total Br}} \times 100\% = \frac{(W_1/M_n) \times M}{(100 - W_1) \times W_2 \times 10^{-2}} \times 100\%$$

Here, W_1 (%) is the PSt weight percent of the PSt-grafted CNC sample and M_n (g/mol) is the molecular weight of PSt cleaved from PSt-grafted CNC and M is the atomic weight of bromine and W_2 (%) is the weight percent of bromine in the initiator-modified CNC.

2.6. The measurement of bromine in the initiator-modified CNC

The oxygen flask method [36] was utilized for determination of bromine in the initiator-modified CNC. The apparatus consists of a conical flask (500 ml) fitted with a ground-glass stopper, into which is sealed a length of platinum wire. To the end of the wire is attached an oblong of platinum gauze, which acts as a hinge to clamp the sample container. The sodium hydroxide (20 ml, 10 wt%) and 3 drops of hydrogen peroxide were added into flask as the absorption solution. The completely dried sample (0.0265 g) was weighed on to a piece of ash-free filter paper, which was carefully folded and then clamped, with the fuse protruding, into the gauze. The flask was flushed with a fast flow of oxygen for a few seconds. The fuse was ignited in a flame, and the stopper was immediately inserted into the flask. Combustion was completed in a few seconds. The flask was then shaken for about 10 min to ensure complete absorption. The stopper was removed and rinsed, together with the gauze and wire. Adding two drops of phenolphthalein (0.1% in ethanol) as an indicator, the solution was neutralized with nitric acid, and 10 ml excess nitric acid was added. The solution was boiled for 5 min to remove peroxide. The bromide was precipitated with a measured but excessive amount of a standard silver nitrate solution. Adding a ferric salt (iron–ammonium alum) as an indicator, the excess of silver nitrate was determined by titration with a standard solution of ammonium thiocyanate. As long as the solution contains any silver, the ammonium thiocyanate

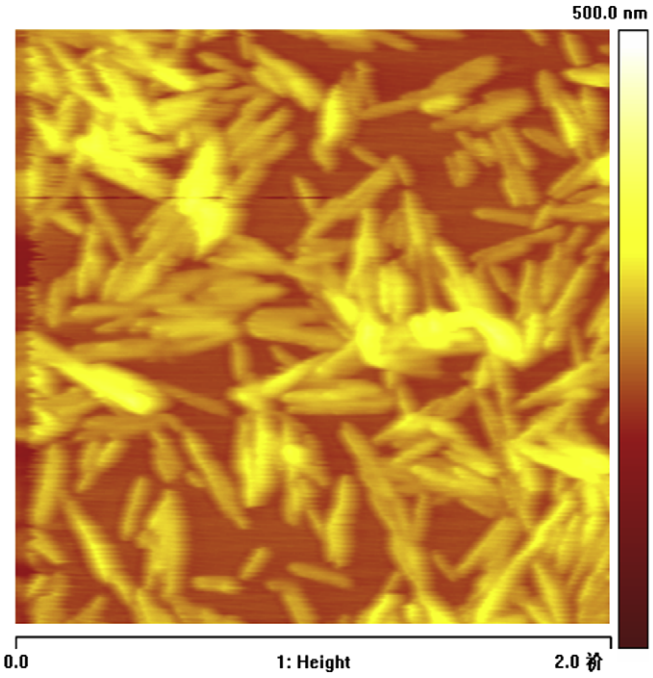

Fig. 1. AFM topography image of rodlike cellulose nanocrystals from a dried water suspension.

produces only a white precipitate of silver thiocyanate. When the solution is colored red by the thiocyanate of iron, the titration endpoints was determined. The blank sample was carried out in the same condition and subtracted from the sample titration. The amount of bromine in the initiator-modified CNC is determined as 0.6 wt%.

2.7. Instruments

DSC was obtained using a Seiko DSC-6200 instrument with a heating rate of 10 °C/min under nitrogen atmosphere from 30 °C to 250 °C.

Thermogravimetric analyses (TGA) were made using a 7 Series thermal analysis system (Perkin–Elmer). Samples were heated at 20 °C/min from room temperature to 600 °C in a dynamic nitrogen atmosphere at a flow rate of 70 ml/min.

FT-IR spectra were recorded on a Perkin–Elmer Spectrum one FTIR spectrophotometer, 64 scans were signal-averaged with a resolution of 2 cm^{-1} at room temperature. Samples were prepared by dispersing the complexes in KBr and compressing the mixtures to form disks.

The atomic force microscopy (AFM) measurements were performed with an AJ-III Atomic Force Microscope. All scans were performed in air with mica. Height images were obtained in tapping mode. The free oscillating amplitude was 3.0 V, while the set point amplitude was chosen individually for each sample. For AFM analysis of cellulose whiskers, a droplet of the aqueous CNC suspension was allowed to dry on a freshly cleaved mica surface.

Polarized optical microscopy (POM) was performed on a Leica DMLP microscope with a Mettler FP82 hot stage. The CNC suspension or PSt-grafted CNC in DMF was transferred into a cavity between slide glasses with a spacer (0.5 mm thick) and observed under POM.

The molecular weights (M_n) and molecular weight distribution (M_w/M_n) were measured on a WATER 2414 gel permeation chromatography (GPC) instrument with a set of HT3, HT4 and HT5, μ-styrayel columns with THF as an eluent (1.0 ml/min) at 35 °C. Calibration was made with standard polystyrene (PSt).

3. Results and discussion

3.1. Morphology of rodlike cellulose nanocrystals

Fig. 1 shows the AFM micrographs of the original microcrystals. The size of the whiskers is 10–40 nm in width and 100–400 nm in length by image analysis. The final ratio is about 10. Dong et al. reported that the whisker size was 7 nm in width and 115 nm in length by transmission electron microscopy (TEM) observation [24]. The difference may be arising from the AFM tips and the individual whiskers agglomeration [37]. In addition, in the drying process, the extra intermolecular hydrogen bonding between crystallites may lead to irreversible aggregation [38]. The irreversible aggregation also may be responsible for the change of the shape of CNC.

3.2. Rodlike cellulose nanocrystals grafted with PSt

Scheme 1 outlines the synthetic pathway for the ATRP polymerization of PSt on the whisker surfaces. The hydroxyl groups on the cellulose nanocrystals were reacted with 2-bromoisobutyryl-bromide for 24 h to yield active ATRP initiators on the surfaces. ATRP was then used to polymerize styrene to the initiated surfaces. Cu(I)Br and the ligand 1,1,4,7,10,10-hexamethyl-triethylenetetramine (HMTETA) were served as catalysts in the ATRP reaction. To ensure complete removal of physically adsorbed, or loosely attached homopolymers, the samples were repeatedly washed and Soxhlet extracted with hot CH_2Cl_2 for a minimum of 48 h. To determine the molecular weight of PSt, the completed PSt chains were cleaved from the CNC surface by HCl hydrolysis. It was necessary to wait for 3 weeks for the complete hydrolysis of the PSt-grafted CNC copolymers due to their highly hydrophobic character. The molecular weights (M_n) and polydispersities of the cleaved PSt were determined using gel permeation chromatography (GPC) (Fig. 2). The number-average molecular weight of the cleaved PSt is 74,700 g/mol. The value of $M_w/M_n = 1.21$ was obtained. By calculating the ratio of the weight of the cleaved PSt to total weight of PSt-grafted CNC, the weight percent of PSt in the PSt-grafted CNC is determined as 68 wt%. The oxygen flask method is available for determining halogens in organic materials. The weight percent of bromine in the initiator-modified CNC is determined as 0.6 wt% by oxygen flask method. The PSt grafting ratio is defined as the ratio of reacted Br to all Br in initiator-modified CNC. According to these experimental data, the PSt grafting ratio is

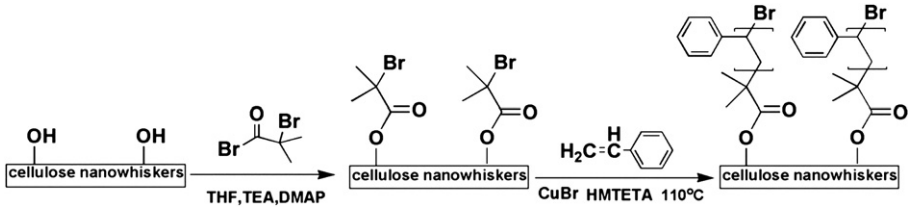

Scheme 1. Formation of PSt grafted on the Rodlike cellulose nanocrystals.

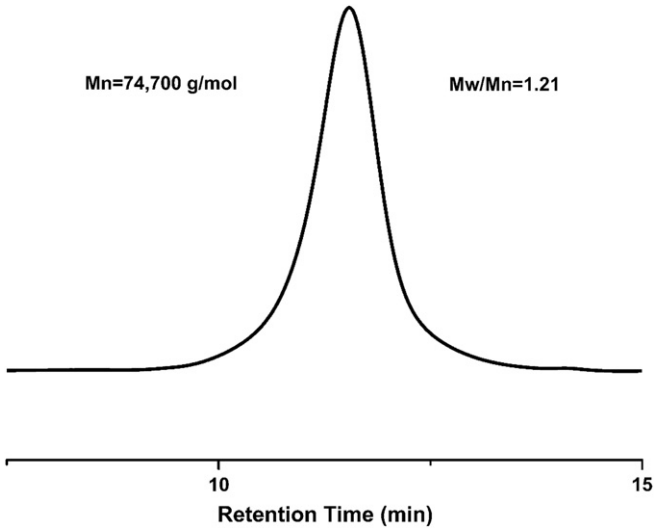

Fig. 2. GPC curve of PSt cleaved from PSt-grafted CNC.

determined as 38%. The value of PSt grafting ratio shows that not all Br initiated styrene polymerization.

FT-IR spectroscopy is well used to characterize cellulose nanocrystals surfaces grafted with polymer [13,39]. Fig. 3 shows the FT-IR spectra of the pure CNC, the initiator-modified CNC and the PSt-grafted CNC. Compared with the pure CNC (Fig. 3a), the FT-IR spectrum of initiator-modified CNC (b) shows a new obvious band for C=O group at 1732 cm^{-1}, demonstrating the successful formation of the CNC initiator. The FT-IR spectra of PSt-grafted CNC (Fig. 3c) show new peaks at 3059, 3025, 1601, 1493, 1452, 756, and 696 cm^{-1}, which are characteristic peaks of poly(styrene) [18]. The aromatic C–H stretching bands for the aromatic ring appear at 3059 and 3025 cm^{-1}. The C=C stretching bands for the aromatic ring appear at 1601, 1493, and 1452 cm^{-1}. The out-of-plane C–H bending mode of the aromatic ring is shown at 756 cm^{-1}. The strong absorption band at 696 cm^{-1} represents the deformation vibration of the –CH– group of the monosubstituted benzene ring in poly(styrene), and confirms the successful grafting between CNC and poly(styrene). The absorption band at about 700 cm^{-1} has also been used as the main proof of grafting and quantitative determination of the poly(styrene) in cotton cellulose–poly(styrene) copolymers [40].

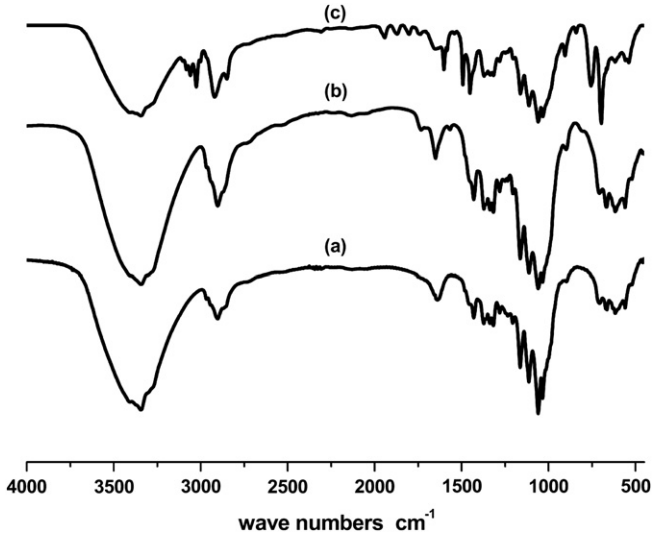

Fig. 3. FT-IR spectra of (a) the pure CNC; (b) the initiator-modified CNC; (c) the PSt-grafted CNC.

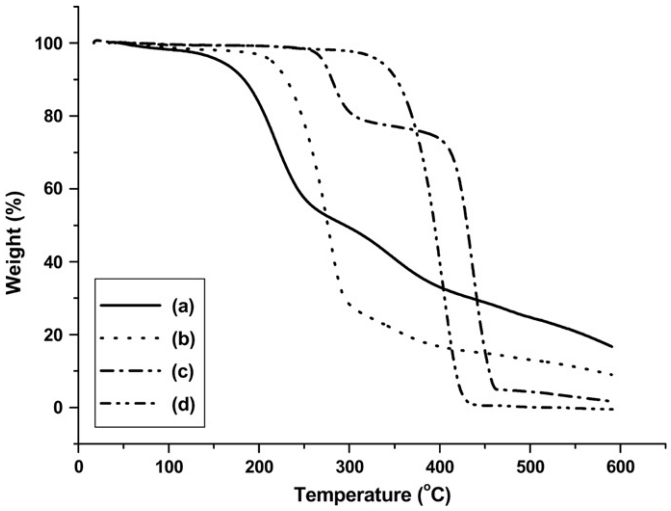

Fig. 4. The thermogravimetry curves of (a) the pure CNC; (b) the initiator-modified CNC; (c) the PSt-grafted CNC; (d) the pure PSt.

3.3. Thermogravimetric analysis

Fig. 4 shows the thermogravimetric curves of (a) the pure CNC, (b) the initiator-modified CNC, (c) the PSt-grafted CNC, and (d) the pure PSt. All samples have a small weight loss in low temperature (<120 °C) range, corresponding to the evaporation of absorbed water. Poly(styrene) decomposes (Fig. 4d) in the range of 360–424 °C with a very small amount of residual mass (0.5 wt%), while the pyrolysis of pure CNC (a) ranges from 320 to 600 °C and yields a higher amount of residual mass (16.7 wt%), mainly due to the formation of levoglucosan [18]. Furthermore, the pure CNC sample degradation shows two separated pyrolysis within a wider temperature range rather than one pyrolysis. It is because that the trace sulfuric acid residue in CNC reduced the degradation temperature of cellulose nanocrystalline. Sulfuric acid was a well-known dehydration catalyst and facilitated the char residue formation. The first process corresponds to the primary pyrolysis of CNC catalyzed by acid sulfate groups, and the second process relate to the slow charring process of the solid residue. The phenomenon is similar to thermal degradation behaviors of spherical cellulose nanocrystals with sulfate groups [41]. In general, thermal decomposition of unmodified cellulose proceeds at 320–360 °C. The thermogravimetric curve of initiator-modified CNC sample (Fig. 4b) shows the decomposition temperature at 233 °C, which was a characteristic of the chemically modified cellulose [42,43]. The present results illustrate the success of the CNC initiator. The trace sulfuric acid residue in CNC was eliminated in the synthesis initiator-modified CNC process. Therefore, the initiator-modified CNC sample almost shows one pyrolysis process. The degradation profile of PSt-grafted CNC (Fig. 4c) contains two steps, the first is due to the degradation of rodlike cellulose nanocrystalline initiator at 265–413 °C and the latter is due to PSt degradation at 413–456 °C with 1.7 wt% char residue at 600 °C. The initial degradation temperature of the PSt-grafted CNC is higher than unmodified CNC, which indicates the increment of the thermal stability of cellulose crystals after grafting. The amount of PSt in the PSt-grafted CNC is determined as 69 wt% by calculating the decrease of PSt weight in the curve (Fig. 4c).

3.4. Liquid crystalline behavior

The phase transitions of the CNC samples were investigated by DSC. Fig. 5 shows the second heating DSC curves of (a) the pure

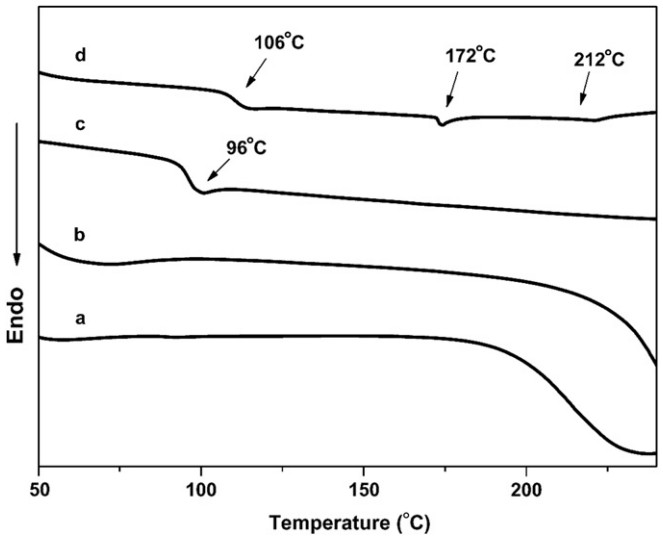

Fig. 5. The DSC curves of (a) CNC; (b) initiator-modified CNC; (c) pure PSt; (d) PSt-grafted CNC.

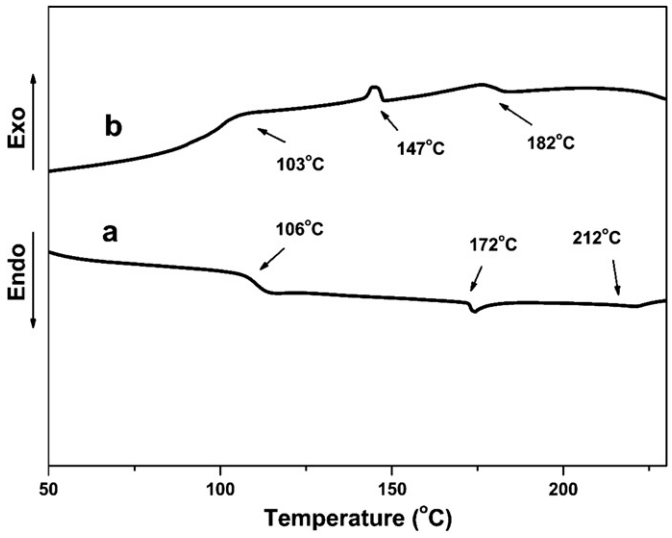

Fig. 6. The DSC curves of PSt-grafted CNC (a) the second heating curve (b) the first cooling curve.

CNC, (b) the initiator-modified CNC, (c) the pure PSt and (d) the PSt-grafted CNC. The DSC curve of the pure CNC shows only a decomposition temperature at 235 °C in the heating scan. Whereas the DSC curve of the initiator-modified CNC shows a decomposition temperature at 250 °C, higher than that of the pure CNC, ascribing to the increment of the thermal stability after grafting 2-bromoisobutyrylbromide. The curve of pure PSt only shows the glass transition of PSt at 96 °C (Fig. 5c). Three endothermic peaks are observed in the DSC curves of PSt-grafted CNC (Fig. 5d), respectively, corresponding to the glass transition of PSt at 106 °C and two liquid crystalline phases transitions at 172 °C and 212 °C. Furthermore, the first cooling DSC curve (Fig. 6b) shows three corresponding exothermic peaks at 103 °C, 147 °C and 182 °C.

Fig. 7 shows the optical micrograph of the pure CNC and PSt-grafted CNC in lyotropic state. The pure CNC water suspension (3.1 wt%) shows fingerprint texture (Fig. 7a). The fingerprint texture is a typical morphology of the chiral-nematic phase (cholesteric phase) [10,20–27]. The pitch measured in our case is 2–3 μm, which is close to the reported value in cyclohexane suspension [10]. However, the spherulitic structures are observed in the zone of isotropic and anisotropic phases equilibrium of PSt-grafted CNC DMF suspension (5.7 wt%) (Fig. 7b), which have not been observed in modified CNC suspension before. The spherulitic structure is the characteristic of cholesteric phase [44,45]. The series of light and dark rings observed within the spherulites correspond to the arrangement of cholesteric planes, in which the helix axis lies in the micrograph plane. The distance between two consecutive rings is thus equal to half the helical pitch *P* of the structure. To lyotropic cholesteric LC solution, the spherulites texture is governed by the surface energy between the isotropic and anisotropic phases, and the cumulative twist is not developed until the droplets coalesce. With increasing concentration, more PSt-grafted CNC congregate in the anisotropic phase and other advanced textures is consequently formed, such as the fingerprint texture (Fig. 7c) and the spherulite texture disappears, which due to the surface tension is too weak to keep the LC phase in the round shape. Fig. 7c compared with Fig. 7a, the defects or imperfections are also important features in the fingerprint texture, such as disclinations and dislocations of the cholesteric order. The defects arise from the singularity of the local director of the molecules and the singularity of the helix axis [45] and they are more complicated than those in the nematic state. The pitch in Fig. 7c is 1–2 μm. The value is less than that of Fig. 7a, which is attributable to PSt on the surface of CNC that decreases repulsion range and causes the rods more effective to twist. Inspection of Fig. 7c, clarifies that the dark zone may be PSt aggregate region. It is because PSt prefers to aggregate together resulting in the weakness of refraction.

Fig. 8 shows the PSt-grafted CNC image of POM in the first cooling and the second heating scan. The CNC is not a thermotropic material. Surprisingly, the PSt-grafted CNC shows the fingerprint texture (Fig. 8b) arising from the cholesteric phase when the PSt-grafted CNC is cooled to 163 °C. It is because the PSt-grafted CNC

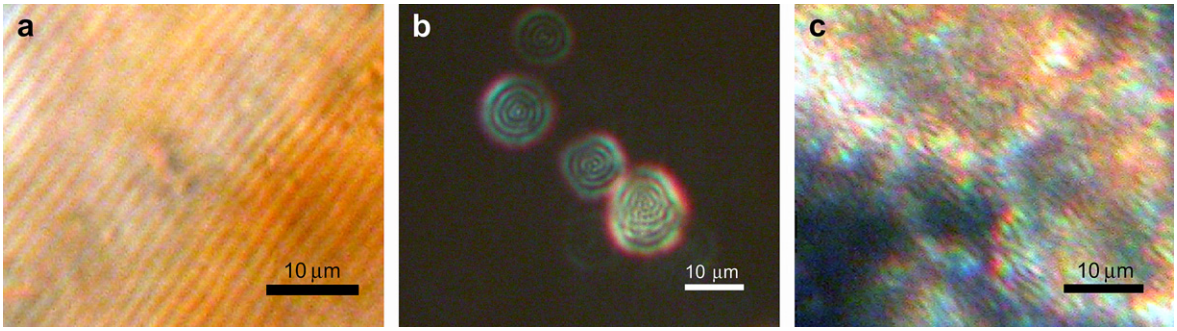

Fig. 7. Optical micrograph (crossed polars): (a) the fingerprint texture of pure CNC suspension (3.1 wt%); (b) the spherulitic structures in the zone of isotropic and anisotropic phases equilibrium of PSt-grafted CNC suspension (5.7 wt%); (c) the fingerprint texture in the zone of anisotropic phase of PSt-grafted CNC suspension (5.7 wt%).

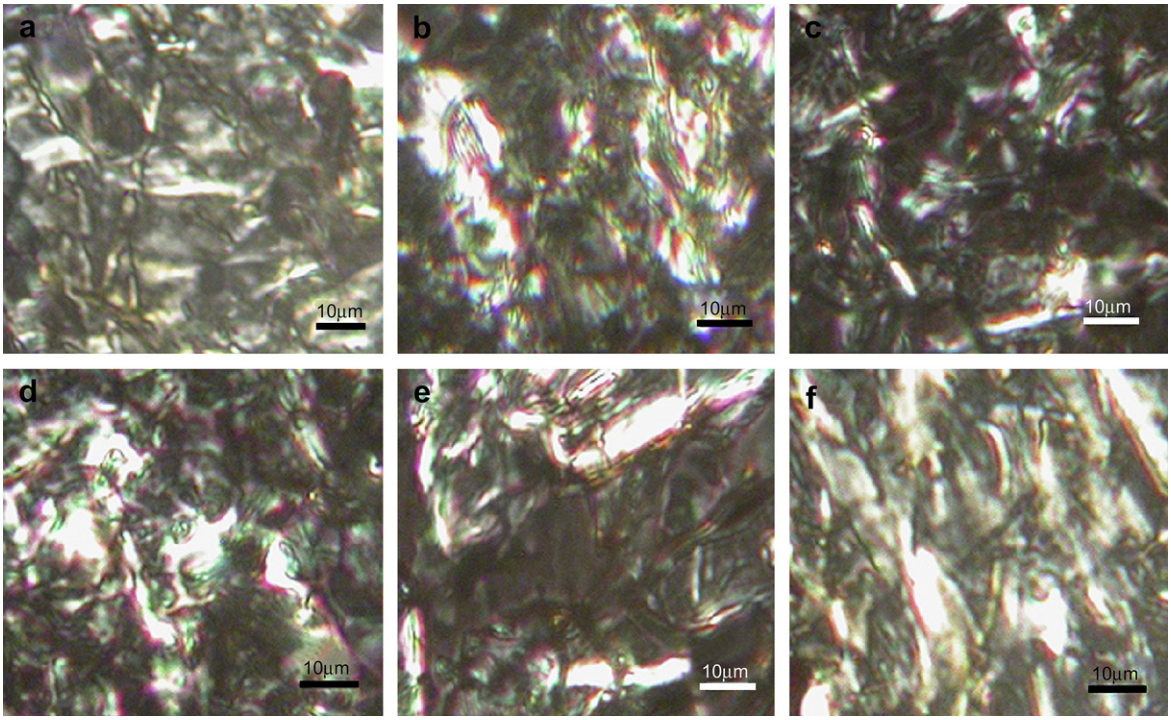

Fig. 8. The POM image of the first cooling from (a)–(c): (a) 226 °C; (b) 163 °C; (c) 138 °C and the POM image of the second heating from (d)–(f): (d) 120 °C; (e) 179 °C; (f) 224 °C.

orients spontaneously in isotropic melt (PSt side chains acting as a solvent). The behavior is similar to that of poly(γ-*n*-alkyl D-glutamate)s having long alkyl side chains above the T_m of the alkyl (long alkyl side chains acting as a solvent) group [33]. The films of PSt-grafted CNC show birefringence above the melting temperature of the side chains (PSt side chains acting as a solvent). To our knowledge, this is the first instance of spontaneous chiral-nematic phase of CNC at thermotropic state. Increasing with temperature, the fingerprint texture is decreased. The liquid crystalline phases transition behavior in thermotropic states will require more detailed investigations including X-ray diffraction, and rheological experiments.

Previous studies suggested possible origins of chiral ordering may be the cause of geometric twists in the microcrystals [20,25,46] or helical distribution of surface charge [20]. Heux et al. found a chiral-nematic order in a cellulose microcrystal system sterically stabilized in toluene, concluding that the chirality originates from the twisted geometry of particles [10]. Araki et al. also prepared another type of sterically stabilized cellulose microcrystals by grafting poly(ethylene glycol) [11]. All that provided more evidence for the role of twists in a particle shape. Our results are consistent with the hypothesis of a chiral interaction arising from the shape of the rods and not from the chiral character of the cellulose chain.

4. Conclusion

In this work, we successfully grafted rodlike cellulose nanocrystals with styrene by ATRP. The PSt-grafted CNC exhibits the chiral-nematic structure in both the thermotropic and the lyotropic states. It is the first instance of exhibiting chiral-nematic liquid crystalline phase of chemically modified rodlike cellulose nanocrystals in both the thermotropic and the lyotropic states. Our results are consistent with the hypothesis of a chiral interaction arising from the shape of the rods and not from the chiral character of the cellulose chain. However, the liquid crystalline phases transition behavior in thermotropic states will require more detailed investigations.

5. Acknowledgments

This work was financially supported by the New Century Excellent Talents in University (NCET-05-0707), the Scientific Research Fund of Hunan Provincial Education Department (06A068), the Cultivation Fund of the Key Scientific and Technical Innovation Project, Ministry of Education of China (No. 207075) and the open Project Program of Key Laboratory of Low-Dimensional Materials and Application Technology of Ministry of Education.

References

[1] de Souza Lima MM, Borsali R. Macromol Rapid Commun 2004;25:771–87.
[2] Samir MASA, Alloin F, Dufresne A. Biomacromolecules 2005;6:612–26.
[3] Sturcova A, Davies GR, Eichhorn SJ. Biomacromolecules 2005;6:1055–61.
[4] Helbert W, Cavaille JY, Dufresne A. Polym Compos 1996;17:604–11.
[5] Battista OA, Coppick S, Howsmon JA, Morehead FF, Sisson WA. Ind Eng Chem 1955;48:333–5.
[6] Marchessault RH, Morehead FF, Koch MJ. J Colloid Sci 1961;16:327–44.
[7] Dong XM, Revol J-F, Gray DG. Cellulose 1998;5:19–32.
[8] Beck-Candanedo S, Roman M, Gray DG. Biomacromolecules 2005;6:1048–54.
[9] Mohanty AK, Misra M, Drzal LT. Compos Interfaces 2001;8:313–44.
[10] Heux L, Chauve G, Bonini C. Langmuir 2000;16:8210–2.
[11] Araki J, Wada M, Kuga S. Langmuir 2001;17:21–7.
[12] Goussé C, Chanzy H, Excoffier G, Soubeyrand L, Fleury E. Polymer 2002;43(9):2645–51.
[13] Carlmark A, Malmström E. J Am Chem Soc 2002;124:900–1.
[14] Carlmark A, Malmström E. Biomacromolecules 2003;4:1740–5.
[15] Lee SB, Koepsel RR, Morley SW, Matyjaszewski K, Sun Y, Russell AJ. Biomacromolecules 2004;5:877–82.
[16] Coskun M, Temüz MM. Polym Int 2005;54(2):342–7.
[17] Lindqvist J, Malmström E. J Appl Polym Sci 2006;100:4155–62.
[18] Roy D, Guthrie JT, Perrier S. Macromolecules 2005;38:10363–72.
[19] Barsbay M, Gu1ven O, Stenzel MH, Davis TP, Barner-Kowollik C, Barner L. Macromolecules 2007;40:7140–7.
[20] Revol J-F, Bradford H, Giasson J, Marchessault RH, Gray DG. Int J Biol Macromol 1992;14:170–2.
[21] Revol JF, Godbout L, Dong XM, Gray DG, Chanzy H, Maret G. Liq Cryst 1994;16:127–34.
[22] Araki J, Kuga S. Langmuir 2001;17:4493–6.

[23] Bercea M, Navard P. Macromolecules 2000;33:6011–6.
[24] Dong XM, Kimura T, Revol J-F, Gray DG. Langmuir 1996;12:2076–82.
[25] Orts WJ, Godbout L, Marchessault RH, Revol J-F. Macromolecules 1998;31:5717–25.
[26] Araki J, Wada M, Kuga S, Okano T. Langmuir 2000;16:2413–5.
[27] Marchessault RH, Morehead FF, Walter NM. Nature 1959;184:632–3.
[28] Onsager L. Ann NYAcad Sci 1949;51:627–59.
[29] Flory PJ. Proc R Soc London Ser A 1956;254:73–89.
[30] Flory PJ, Ronca G. Mol Cryst Liq Cryst 1979;54:289–310.
[31] Petekidis G, Vlassopoulos D, Fytas G, Kountourakis N. Macromolecules 1997;30:919–31.
[32] Kricheldorf HR, Wahlen LH. Macromolecules 1997;30:2642–50.
[33] Sakamoto R, Osawa A. Mol Cryst Liq Cryst 1987;153(1):385–94.
[34] Bouteiller L, Barny PL. Liq Cryst 1996;21:157–74.
[35] Fleming K, Gray DG, Matthews S. Chem Eur J 2001;7(9):1831–5.
[36] MacDonald AMG. Analyst 1961;86:3–12.
[37] Kvien I, Tanem BS, Oksman K. Biomacromolecules 2005;6(6):3160–5.
[38] Dong XM, Gray DG. Langmuir 1997;13:2404–9.
[39] Plackett D, Jankova K, Egsgaard H, Hvilsted S. Biomacromolecules 2005;6:2474–84.
[40] Imrisova D, Maryska S. J Appl Polym Sci 1968;12:2007–11.
[41] Wang N, Ding E, Cheng R. Polymer 2007;48:3486–93.
[42] Varma AJ, Chavan VB. Cellulose 1995;2:41–9.
[43] Lerdkanchanaporn S, Dollimore D, Alexander KS. Thermochim Acta 1998;324:25–32.
[44] Patel DL, Dupré DB. J Polym Sci Polym Phys Ed 1980;18:1599–607.
[45] Wang L, Huang Y. Macromolecules 2004;37:303–9.
[46] Revol J-F, Marchessault RH. Int J Biol Macromol 1993;15:329–35.